
WHAT DO COMPRESSED DEEP NEURAL NETWORKS FORGET?

Sara Hooker*
Google Brain

Aaron Courville
MILA

Gregory Clark
Google

Yann Dauphin
Google Brain

Andrea Frome
Google Brain

ABSTRACT

Deep neural network pruning and quantization techniques have demonstrated it is possible to achieve high levels of compression with surprisingly little degradation to test set accuracy. However, this measure of performance conceals significant differences in how different classes and images are impacted by model compression techniques. We find that models with radically different numbers of weights have comparable top-line performance metrics but diverge considerably in behavior on a narrow subset of the dataset. This small subset of data points, which we term Pruning Identified Exemplars (PIEs), are systematically more impacted by the introduction of sparsity. Our work is the first to provide a formal framework for auditing the disparate harm incurred by compression and a way to quantify the trade-offs involved. An understanding of this disparate impact is critical given the widespread deployment of compressed models in the wild.

1 Introduction

Between infancy and adulthood, the number of synapses in our brain first multiply and then fall. Synaptic pruning improves efficiency by removing redundant neurons and strengthening synaptic connections that are most useful for the environment (Rakic et al., 1994). Despite losing 50% of all synapses between age two and ten, the brain continues to function (Kolb & Whishaw, 2009; Sowell et al., 2004). The phrase "Use it or lose it" is frequently used to describe the environmental influence of the learning process on synaptic pruning, however there is little scientific consensus on *what* exactly is lost (Casey et al., 2000).

In this work, we ask what is *lost* when we compress a deep neural network. Work since the 1990s has shown that deep neural networks can be pruned of "excess capacity" in a similar fashion to synaptic pruning (Cun et al., 1990; Hassibi et al., 1993a; Nowlan & Hinton, 1992; Weigend et al., 1991). At face value, compression appears to promise you can have it all. Deep neural networks are remarkably tolerant of high levels of pruning and quantization with an almost negligible loss to top-1 accuracy (Han et al., 2015; Ullrich et al., 2017; Liu et al., 2017; Louizos et al., 2017; Collins & Kohli, 2014; Lee et al., 2018). These more compact networks are frequently favored in resource constrained settings; compressed models require less memory, energy consumption and have lower inference latency (Reagen et al., 2016; Chen et al., 2016; Theis et al., 2018; Kalchbrenner et al., 2018; Valin & Skoglund, 2018; Tessler et al., 2021).

The ability to compress networks with seemingly so little degradation to generalization performance is puzzling. How can networks with radically different representations and number of parameters have comparable top-level metrics? One possibility is that test-set accuracy is simply not a precise enough measure to capture how compression impacts the generalization properties of the model. Despite the widespread use of compression techniques, articulating the trade-offs of compression has overwhelmingly focused on change to overall top-1 accuracy for a given level of compression.

The cost to top-1 accuracy appears minimal if it is spread uniformly across all classes, but what if the cost is concentrated in only a few classes? *Are certain types of examples or classes disproportionately*

*Correspondence should be directed to shooker@google.com

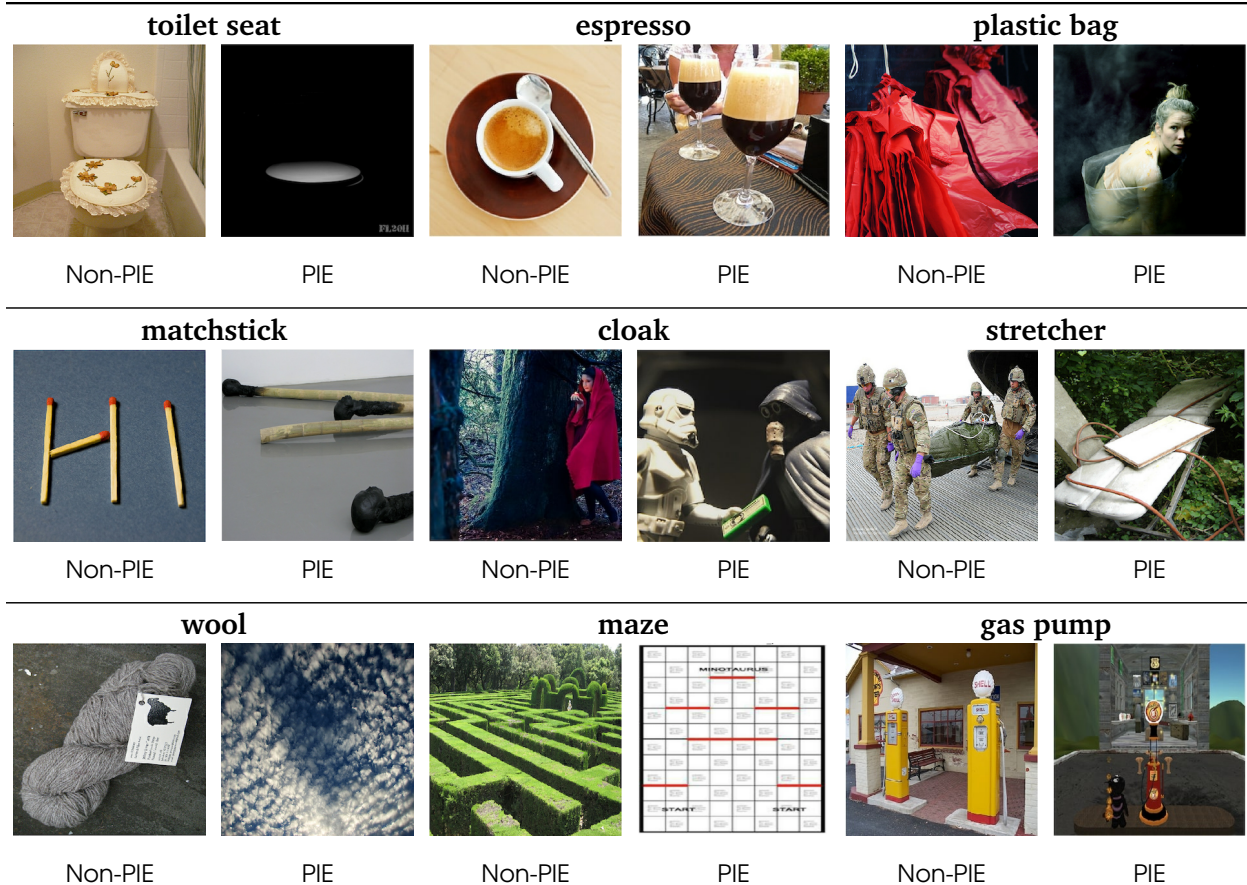


Figure 1: Pruning Identified Exemplars (PIEs) are images where there is a high level of disagreement between the predictions of pruned and non-pruned models. Visualized are a sample of ImageNet PIEs alongside a non-PIE image from the same class. Above each image pair is the true label.

impacted by compression? In this work, we propose a formal framework to audit the impact of compression on generalization properties beyond top-line metrics. Our work is the first to our knowledge that asks how dis-aggregated measures of model performance at a class and exemplar level are impacted by compression.

Contributions We run thousands of large scale experiments and establish consistent results across multiple datasets— CIFAR-10 (Krizhevsky, 2012), CelebA (Liu et al., 2015) and ImageNet (Deng et al., 2009), widely used pruning and quantization techniques, and model architectures. We find that:

1. Top-line metrics such as top-1 or top-5 test-set accuracy hide critical details in the ways that pruning impacts model generalization. Certain parts of the data distribution are far more sensitive to varying the number of weights in a network, and bear the brunt of the cost of varying the weight representation.
2. The examples most impacted by pruning, which we term *Pruning Identified Exemplars (PIEs)*, are more challenging for both models and humans to classify. We conduct a human study and find that PIEs tend to be mislabelled, of lower quality, depict multiple objects, or require fine-grained classification. Compression impairs the model’s ability to predict accurately on the long-tail of less frequent instances.
3. Pruned networks are more sensitive to natural adversarial images and corruptions. This sensitivity is amplified at higher levels of compression.
4. While all compression techniques that we evaluate have a non-uniform impact, not all methods are created equal. High levels of pruning incur a far higher disparate impact than is observed for the quantization techniques that we evaluate.

Our work provides intuition into the role of capacity in deep neural networks and a mechanism to audit the trade-offs incurred by compression. Our findings suggest that caution should be used before deploying compressed networks to sensitive domains. Our PIE methodology could conceivably be explored as a mechanism to surface a tractable subset of atypical examples for further human inspection (Leibig et al., 2017; Zhang, 1992), to choose not to classify certain examples when the model is uncertain (Bartlett & Wegkamp, 2008; Cortes et al., 2016), or to aid interpretability as a case based reasoning tool to explain model behavior (Kim et al., 2016; Caruana, 2000; Hooker et al., 2019).

2 Methodology and Experiment Framework

2.1 Preliminaries

We consider a supervised classification problem where a deep neural network is trained to approximate the function F that maps an input variable X to an output variable Y , formally $F : X \mapsto Y$. The model is trained on a training set of N images $\mathcal{D} = \{(x_i, y_i)\}_{i=1}^N$, and at test time makes a prediction y_i^* for each image in the test set. The true labels y_i are each assumed to be one of C classes, such that $y_i = [1, \dots, C]$.

A reasonable response to our desire for more compact representations is to simply train a network with fewer weights. However, as of yet, starting out with a compact dense model has not yielded competitive test-set performance (Li et al., 2020; Zhu & Gupta, 2017b). Instead, research has centered on a more tractable direction of investigation – the model begins training with "excess capacity" and the goal is to remove the parts that are not strictly necessary for the task by/at the end of training. A pruning method \mathcal{P} identifies the subset of weights to set to zero. A sparse model function, \hat{f}_t^p , is one where a fraction t of all model weights are set to zero. Equating weight value to zero effectively removes the contribution of a weight, as multiplication with inputs no longer contributes to the activation. A non-compressed model function is one where all weights are trainable ($t = 0$). We refer to the overall model accuracy as β_t^M . In contrast, $t = 0.9$ indicates that 90% of model weights are removed over the course of training, leaving a maximum of 10% non-zero weights.

2.2 Class level measure of impact

If the impact of compression was completely uniform, the relative relationship between class level accuracy β_t^c and overall model performance will be unaltered. This forms our null hypothesis (H_0). We must decide for each class c whether to reject the null hypothesis and accept the alternate hypothesis (H_1) - the relative change to class level recall differs from the change to overall accuracy in either a positive or negative direction:

$$H_0 : \frac{\beta_0^c}{\beta_0^M} = \frac{\beta_t^c}{\beta_t^M} \quad (1)$$

$$H_1 : \frac{\beta_0^c}{\beta_0^M} \neq \frac{\beta_t^c}{\beta_t^M} \quad (2)$$

Welch’s t-test Evaluating whether the difference between the samples of mean-shifted class accuracy from compressed and non-compressed models is “real” amounts to determining whether these two data samples are drawn from the same underlying distribution, which is the subject of a large body of goodness of fit literature (D’Agostino & Stephens, 1986; Anderson & Darling, 1954; Huber-Carol et al., 2002). We independently train a population of K models for each compression method, dataset, and model that we consider. Thus, we have a sample S_t^c of accuracy metrics per class c at each level of compression t .

For each class c , we use a two-tailed, independent Welch’s t-test (Welch, 1947) to determine whether the mean-shifted class accuracy $S_t^c = \{\beta_{t,k}^c - \beta_{t,k}^M\}_{k=1}^K$ of the samples S_t^c and S_0^c differ significantly. If the p -value ≤ 0.05 , we reject the null hypothesis and consider the class to be disparately impacted by t level of compression relative to the baseline.

Controlling for overall changes to top-line metrics Note that by comparing the relative difference in class accuracy S_t^c , we control for any overall difference in model test-set accuracy. This is important because while

small, the difference in top-line metrics is not zero (see Table. 2). Along with the p -value, for each class we report the average relative deviation in class-level accuracy, which we refer to as *relative recall difference*:

$$\frac{1}{K} \sum_{k=1}^K \left(\frac{\beta_{t,k}^c}{\beta_{0,k}^c} \right) \quad (3)$$

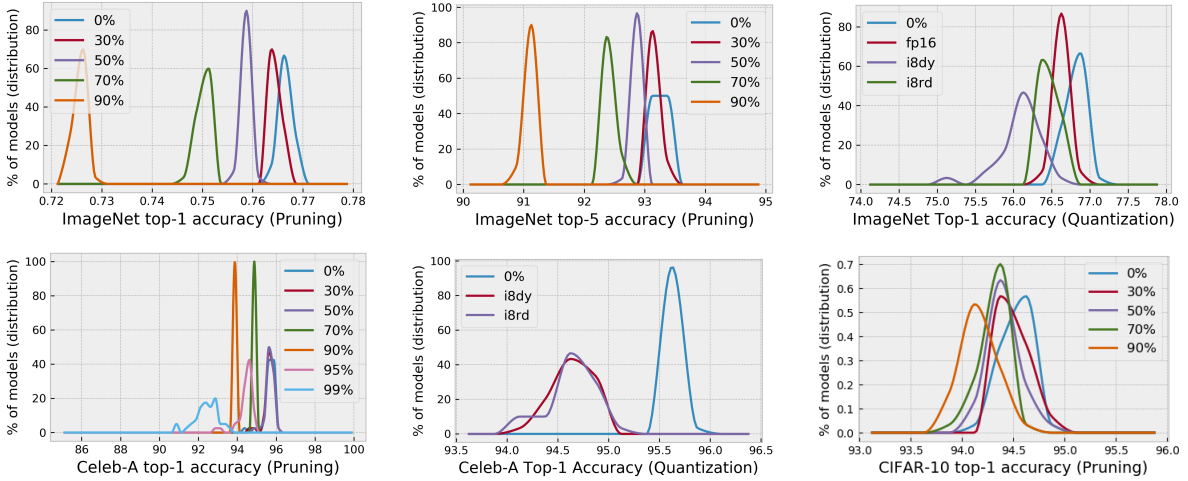


Table 1: Distributions of top-1 accuracy for populations of independently quantized and pruned models for ImageNet, CIFAR-10 and CelebA. For ImageNet, we also include top-5. Note that the scale of the x-axis differs between plots.

2.3 Pruning Identified Exemplars

In addition to measuring the class level impact of compression, we are interested in how model predictive behavior changes through the compression process. Given the limitations of un-calibrated probabilities in deep neural networks (Guo et al., 2017; Kendall & Gal, 2017), we focus on the level of disagreement between the predictions of compressed and non-compressed networks on a given image. Using the populations of models K described in the prior section, we construct sets of predictions $Y_{i,t}^* = \{y_{i,k,t}^*\}_{k=1}^K$ for a given image i .

For set $Y_{i,t}^*$ we find the *modal label*, i.e. the class predicted most frequently by the t -pruned model population for image i , which we denote $y_{i,t}^M$. The exemplar is classified as a pruning identified exemplar PIE_t if and only if the modal label is different between the set of t -pruned models and the non-pruned baseline models:

$$PIE_{i,t} = \begin{cases} 1 & \text{if } y_{i,0}^M \neq y_{i,t}^M \\ 0 & \text{otherwise} \end{cases}$$

We note that there is no constraint that the non-pruned predictions for PIEs match the true label. Thus the detection of PIEs is an unsupervised protocol that can be performed at test time.

2.4 Experimental framework

Tasks We evaluate the impact of compression across three classification tasks and models: a wide ResNet model (Zagoruyko & Komodakis, 2016) trained on CIFAR-10, a ResNet-50 (He et al., 2015) trained on ImageNet, and a ResNet-18 trained on CelebA. All networks are trained with batch normalization (Ioffe & Szegedy, 2015), weight decay, decreasing learning rate schedules, and augmented training data. We train for 32,000 steps (approximately 90 epochs) on ImageNet with a batch size of 1024 images, for 80,000 steps on CIFAR-10 with a batch size of 128, and 10,000 steps on CelebA with a batch size of 256. For ImageNet,

CIFAR-10 and CelebA, the baseline non-compressed model obtains a mean top-1 accuracy of 76.68%, 94.35% and 94.73% respectively. Our goal is to move beyond anecdotal observations, and to measure statistical deviations between populations of models. Thus, we report metrics and statistical significance for each dataset, model and compression variant across 30 independent trainings.

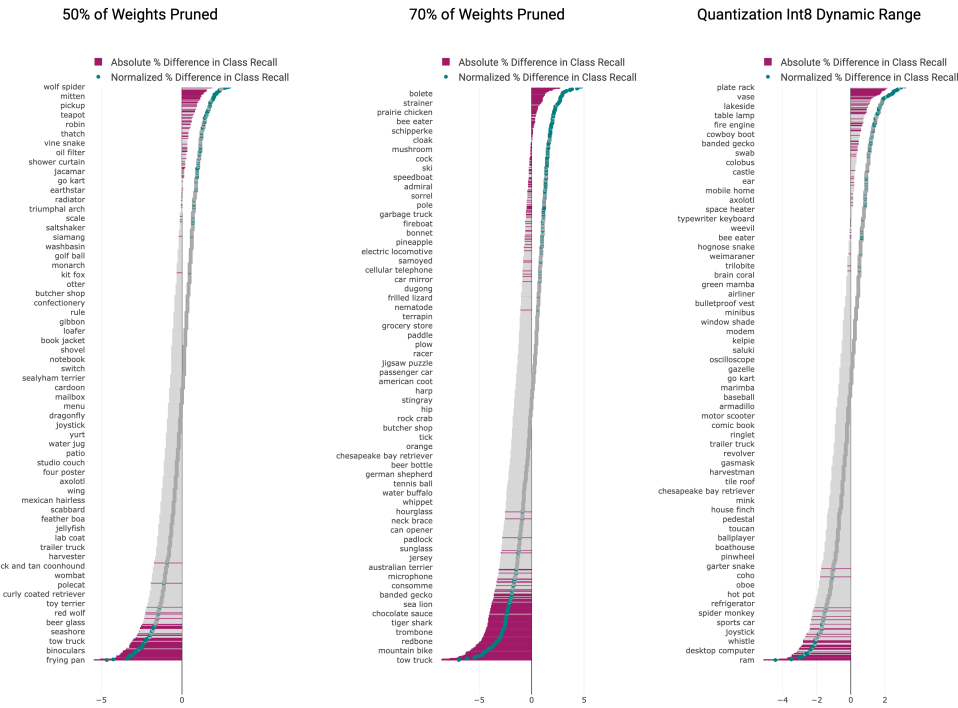


Figure 2: Compression disproportionately impacts a small subset of ImageNet classes. Plum bars indicate the subset of examples where the impact of compression is statistically significant. Green scatter points show normalized recall difference which normalizes by overall change in model accuracy, and the bars show absolute recall difference. **Left:** 50% pruning. **Center:** 70% pruning. **Right:** post-training int8 dynamic range quantization. The class labels are sampled for readability.

Pruning and quantization techniques considered We evaluate magnitude pruning as proposed by Zhu & Gupta (2017a). For pruning, we vary the end sparsity precisely for $t \in \{0.3, 0.5, 0.7, 0.9\}$. For example, $t = 0.9$ indicates that 90% of model weights are removed over the course of training, leaving a maximum of 10% non-zero weights. For each level of pruning t , we train 30 models from random initialization.

We evaluate three different quantization techniques: float16 quantization float16 (Micikevicius et al., 2017), hybrid dynamic range quantization with int8 weights hybrid (Alvarez et al., 2016) and fixed-point only quantization with int8 weights created with a small representative dataset fixed-point (Vanhoucke et al., 2011; Jacob et al., 2018).

All quantization methods we evaluate are implemented post-training, in contrast to the pruning which is applied progressively over the course of training. We use a limited grid search to tailor the pruning schedule and hyperparameters to each dataset to maximize top-1 accuracy. We include additional details about training methodology and pruning techniques in the supplementary material. All the code for this paper is publicly available here.

3 Results

3.1 Disparate impact of compression

We find consistent results across all datasets and compression techniques considered; a small subset of classes are disproportionately impacted. This disparate impact is far from random, with statistically significant differences in class level recall between a population of non-compressed and compressed models. Compression induces “*selective forgetting*” with performance on certain classes evidencing far more sensitivity to varying the representation of the network. This sensitivity is amplified at higher levels of sparsity with more classes evidencing a statistically significant relative change in recall. For example, as seen in Table 2 at 50% sparsity 170 ImageNet classes are statistically significant which increases to 372 classes at 70% sparsity.

Cannibalizing a small subset of classes Out of the classes where there is a statistically significant deviation in performance, we observe a subset of classes that benefit relative to the average class as well as classes that are impacted adversely. However, the average absolute class decrease in recall is far larger than the average increase, meaning that the losses in generalization caused by pruning is far more concentrated than the relative gains. Compression cannibalizes performance on a small subset of classes to preserve a similar overall top-line accuracy.

Comparison of quantization and pruning techniques While all the techniques we benchmark evidence disparate class level impact, we note that quantization appears to introduce less disparate harm. For example, the most aggressive form of post-training quantization considered, fixed-point only quantization with int8 weights fixed-point, impacts the *relative recall difference* of 119 ImageNet classes in a statistically significant way. In contrast, at 90% sparsity, *relative recall difference* is statistically significant for 637 classes. These results suggest that the representation learnt by a network is far more robust to changes in precision versus removing the weights entirely. For sensitive tasks, quantization may be more viable for practitioners as there is less systematic disparate impact.

Complexity of task The impact of compression depends upon the degree of overparameterization present in the network given the complexity of the task in question. For example, the ratio of classes that are significantly impacted by pruning was lower for CIFAR-10 than for ImageNet. One class out of ten was significantly impacted at 30% and 50%, and two classes were impacted at 90%. We suspect that we measured less disparate impact for CIFAR-10 because, while the model has less capacity, the number of weights is still sufficient to model the limited number of classes and lower dimensional dataset. In the next section, we leverage PIEs to characterize and gain intuition into why certain parts of the distribution are systematically far more sensitive to compression.

3.2 Pruning Identified Exemplars

To better understand why a narrow part of the data distribution is far more sensitive to compression, we (1) evaluate whether PIEs are more difficult for an algorithm to classify, (2) conduct a human study to codify the attributes of a sample of PIEs and Non-PIEs, and (3) evaluate whether PIEs over-index on underrepresented sensitive attributes in CelebA.

At every level of compression, we identify a subset of PIE images that are disproportionately sensitive to the removal of weights (for each of CIFAR-10, CelebA and ImageNet). The number of images classified as PIE increases with the level of pruning. At 90% sparsity, we classify 10.27% of all ImageNet test-set images as PIEs, 2.16% of CIFAR-10, and 16.17% of CelebA.

Test-error on PIEs In Fig. 3, we evaluate a random sample of (1) PIE images, (2) non-PIE images and (3) entire test-set for each of the datasets considered. We find that PIE images are far more challenging for a non-compressed model to classify. Evaluation on PIE images alone yields substantially lower top-1 accuracy. The results are consistent across CIFAR-10 (top-1 accuracy falls from 94.89% to 43.64%), CelebA (94.10% to 50.41%), and ImageNet datasets (76.75% to 39.81%). Notably, on ImageNet, we find that removing PIEs greatly improves generalization performance. Test-set accuracy on non-PIEs increased to 81.20% relative to baseline top-1 performance of 76.75%.

FRACTION PRUNED	TOP 1	TOP 5	COUNT SIGNIF CLASSES	COUNT PIEs
0	76.68	93.25	-	-
30	76.46	93.17	68	1,819
50	75.87	92.86	170	2,193
70	75.02	92.43	372	3,073
90	72.60	91.10	637	5,136
QUANTIZATION				
FLOAT16	76.65	93.25	58	2019
DYNAMIC RANGE INT8	76.10	92.94	144	2193
FIXED-POINT INT8	76.46	93.16	119	2093

Table 2: ImageNet top-1 and top-5 accuracy at all levels of pruning and quantization, averaged over all runs. Count PIEs is the count of images classified as a Pruning Identified Exemplars at every compression level. We include comparable tables for CelebA and CIFAR-10 in the appendix.

Human study We conducted a human study (85 participants) to label a random sample of 1230 PIE and non-PIE ImageNet images. Humans in the study were shown a balanced sample of PIE and non-PIE images that were selected at random and shuffled. The classification as PIE or non-PIE was not known or available to the human. *What makes PIEs different from non-PIEs?* The participants were asked to codify a set of attributes for each image. We report the relative distribution of PIE and non-PIE after each attribute, with the higher relative share in bold:

1. **ground truth label incorrect or inadequate** – image contains insufficient information for a human to arrive at the correct ground truth label. [8.90% of non-PIEs, **20.05%** of PIEs]
2. **multiple-object image** – image depicts multiple objects where a human may consider several labels to be appropriate (e.g., an image which depicts both a paddle and canoe or a desktop computer consisting of a screen, mouse, and monitor). [39.53% of non-PIE, **59.15%** of PIEs]
3. **corrupted image** – image exhibits common corruptions such as motion blur, contrast, pixelation. We also include in this category images with super-imposed text or an artificial frame as well as images that are black and white rather than the typical RGB color images in ImageNet. [**14.37%** of non-PIE, 13.72% of PIEs]
4. **fine grained classification** – image involves classifying an object that is semantically close to various other class categories present in the dataset (e.g., rock crab and fiddler crab, bassinet and cradle, cuirass and breastplate). [8.9% of non-PIEs, **43.55%** of PIEs]
5. **abstract representations** – image depicts a class object in an abstract form such a cartoon, painting, or sculptured incarnation of the object. [3.43% of non-PIE, **5.76%** of PIE]

PIEs heavily over-index relative to non-PIEs on certain properties, such as having an *incorrect ground truth label*, involving a *fine-grained classification task* or *multiple objects*. This suggests that the task itself is often incorrectly specified. For example, while ImageNet is a single image classification tasks, 59% of ImageNet PIEs codified by humans were identified as multi-object images where multiple labels could be considered reasonable (vs. 39% of non-PIEs). In ImageNet, the over-indexing of incorrectly labelled data and multi-object images in PIE also raises questions about whether the explosion of growth in number of weights in deep neural networks is solving a problem that is better addressed in the data cleaning pipeline.

4 Sensitivity of compressed models to distribution shift

Non-compressed models have already been shown to be very brittle to small shifts in the distribution that humans are robust. This can cause unexpected changes in model behavior in the wild that can compromise human welfare (Zech et al., 2018). Here, we ask *does compression amplify this brittleness?* Understanding relative differences in robustness helps understand the implications for AI safety of the widespread use of compressed models.

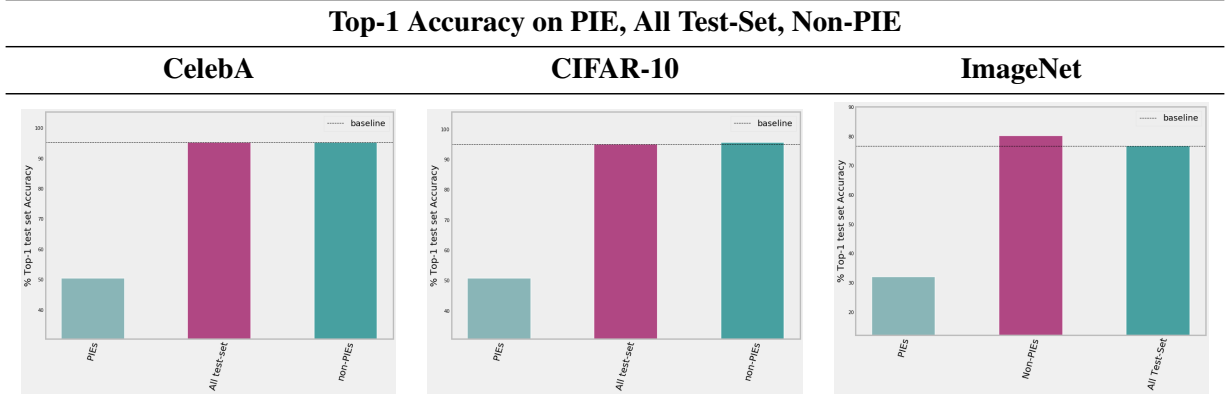


Figure 3: A comparison of model performance on 1) a sample of Pruning Identified Exemplars (PIE), 2) the entire test-set and 3) a sample excluding PIEs. Inference on the non-PIE sample improves test-set top-1 accuracy relative to the baseline for ImageNet. Evaluation on PIE images alone yields substantially lower top-1 accuracy.

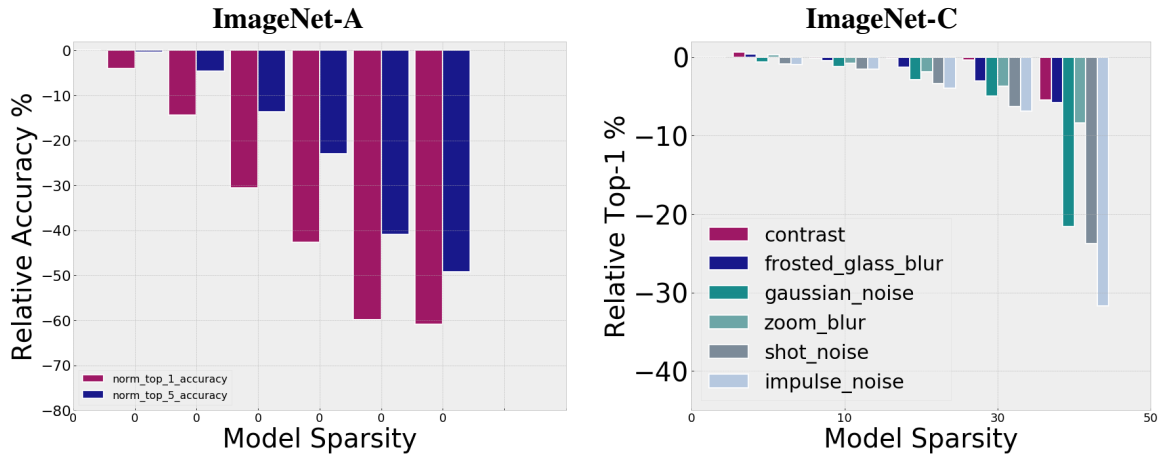


Figure 4: High levels of compression amplify sensitivity to distribution shift. **Left:** Change in top-1 and top-5 recall of a pruned model *relative* to a non-pruned model on ImageNet-A. **Right:** We measure the top-1 test-set performance on a subset of ImageNet-C corruptions of a pruned model relative to the non-pruned model on the same corruption. An extended list of all corruptions considered and top-5 accuracy is included in the supplementary material.

To answer this question, we evaluate the sensitivity of pruned models *relative* to non-pruned models given two open-source benchmarks for robustness:

1. **ImageNet-C** (Hendrycks & Dietterich, 2019) – 16 algorithmically generated corruptions (blur, noise, fog) applied to the ImageNet test-set.
2. **ImageNet-A** (Hendrycks et al., 2019) – a curated test set of 7,500 naturally adversarial images designed to produce drastically lower test accuracy.

For each ImageNet-C corruption $q \in Q$, we compare top-1 accuracy of the pruned model evaluated on corruption q normalized by non-pruned model performance on the same corruption. We average across intensities of corruptions as described by Hendrycks & Dietterich (2019). If the relative top-1 accuracy was 0 it would mean that there is no difference in sensitivity to corruptions considered.

As seen in Fig. 4, pruning greatly amplifies sensitivity to both ImageNet-C and ImageNet-A relative to non-pruned performance on the same inputs. For ImageNet-C, it is worth noting that relative degradation

in performance is remarkably varied across corruptions, with certain corruptions such as gaussian, shot noise, and impulse noise consistently causing far higher relative degradation. At $t = 90$, the highest degradation in relative top-1 is shot noise (-40.11%) and the lowest relative drop is brightness (-7.73%). Sensitivity to small distribution shifts is amplified at higher levels of sparsity. We include results for all corruptions and the absolute top-1 and top-5 accuracy on each corruption, level of pruning considered in the supplementary material Table. 8.

The amplified sensitivity of smaller models to distribution shifts and the over-indexing of PIEs on low frequency attributes suggests that much of a model’s excess capacity is helpful for learning features which aid generalization on atypical or out-of-distribution data points. This builds upon recent work which suggests memorization can benefit generalization properties (Feldman & Zhang, 2020).

5 Related work

The set of model compression techniques is diverse and includes research directions such as reducing the precision or bit size per model weight (quantization) (Jacob et al., 2018; Courbariaux et al., 2014; Hubara et al., 2016; Gupta et al., 2015), efforts to start with a network that is more compact with fewer parameters, layers or computations (architecture design) (Howard et al., 2017; Iandola et al., 2016; Kumar et al., 2017), student networks with fewer parameters that learn from a larger teacher model (model distillation) (Hinton et al., 2015) and finally pruning by setting a subset of weights or filters to zero (Louizos et al., 2017; Wen et al., 2016; Cun et al., 1990; Hassibi et al., 1993b; Ström, 1997; Hassibi et al., 1993a; Zhu & Gupta, 2017; See et al., 2016; Narang et al., 2017). In this work, we evaluate the dis-aggregated impact of a subset of pruning and quantization methods.

Despite the widespread use of compression techniques, articulating the trade-offs of compression has overwhelmed centered on change to overall accuracy for a given level of compression (Ström, 1997; Cun et al., 1990; Evci et al., 2019; Narang et al., 2017; Gale et al., 2019). Our work is the first to our knowledge that asks how dis-aggregated measures of model performance at a class and exemplar level are impacted by compression.

In section 4, we also measure sensitivity to two types of distribution shift – ImageNet-A and ImageNet-C. Recent work by (Guo et al., 2018; Schwag et al., 2019) has considered sensitivity of pruned models to a different notion of robustness: $l - p$ norm adversarial attacks. In contrast to adversarial robustness which measures the worst-case performance on targeted perturbation, our results provide some understanding of how compressed models perform on subsets of challenging or corrupted natural image examples. Zhou et al. (2019) conduct an experiment which shows that networks which are pruned subsequent to training are more sensitive to the corruption of labels at training time.

6 Discussion and Future Work

The quantization and pruning techniques we evaluate in this paper are already widely used in production systems and integrated with popular deep learning libraries. The popularity and widespread use of these techniques is driven by the severe resource constraints of deploying models to mobile phones or embedded devices (Samala et al., 2018). Many of the algorithms on your phone are likely pruned or compressed in some way.

Our results suggest that a reliance on top-line metrics such as top-1 or top-5 test-set accuracy hides critical details in the ways that compression impacts model generalization. Caution should be used before deploying compressed models to sensitive domains such as hiring, health care diagnostics, self-driving cars, facial recognition software. For these domains, the introduction of pruning may be at odds with the need to guarantee a certain level of recall or performance for certain subsets of the dataset.

Role of Capacity in Deep Neural Networks A “bigger is better” race in the number of model parameters has gripped the field of machine learning (Canziani et al., 2016; Strubell et al., 2019). However, the role of additional weights is not well understood. The over-indexing of PIEs on low frequency attributes suggest that non-compressed networks use the majority of capacity to encode a useful representation for these examples.

This costly approach to learning an appropriate mapping for a small subset of examples may be better solved in the data pipeline.

Auditing and improving compressed models Our methodology offers one way for humans to better understand the trade-offs incurred by compression and surface challenging examples for human judgement. Identifying harm is the first step in proposing a remedy, and we anticipate our work may spur focus on developing new compression techniques that improve upon the disparate impact we identify and characterize in this work.

Limitations There is substantial ground we were not able to address within the scope of this work. Open questions remain about the implications of these findings for other possible desirable objectives such as fairness. Underserved areas worthy of future consideration include evaluating the impact of compression on additional domains such as language and audio, and leveraging these insights to explicitly optimize for compressed models that *also* minimize the disparate impact on underrepresented data attributes.

Acknowledgements

We thank the generosity of our peers for valuable input on earlier versions of this work. In particular, we would like to acknowledge the input of Jonas Kemp, Simon Kornblith, Julius Adebayo, Hugo Larochelle, Dumitru Erhan, Nicolas Papernot, Catherine Olsson, Cliff Young, Martin Wattenberg, Utku Evci, James Wexler, Trevor Gale, Melissa Fabros, Prajit Ramachandran, Pieter Kindermans, Erich Elsen and Moustapha Cisse. We thank R6 from ICML 2021 for pointing out some improvements to the formulation of the class level metrics. We thank the institutional support and encouragement of Natacha Mainville and Alexander Popper.

References

- Alvarez, R., Prabhavalkar, R., and Bakhtin, A. On the efficient representation and execution of deep acoustic models. *Interspeech 2016*, Sep 2016. doi: 10.21437/interspeech.2016-128. URL <http://dx.doi.org/10.21437/Interspeech.2016-128>.
- Anderson, T. W. and Darling, D. A. A test of goodness of fit. *Journal of the American Statistical Association*, 49(268):765–769, 1954. ISSN 01621459. URL <http://www.jstor.org/stable/2281537>.
- Bartlett, P. L. and Wegkamp, M. H. Classification with a reject option using a hinge loss. *J. Mach. Learn. Res.*, 9:1823–1840, June 2008. ISSN 1532-4435. URL <http://dl.acm.org/citation.cfm?id=1390681.1442792>.
- Canziani, A., Paszke, A., and Culurciello, E. An Analysis of Deep Neural Network Models for Practical Applications. *arXiv e-prints*, art. arXiv:1605.07678, May 2016.
- Caruana, R. Case-based explanation for artificial neural nets. In Malmgren, H., Borga, M., and Niklasson, L. (eds.), *Artificial Neural Networks in Medicine and Biology*, pp. 303–308, London, 2000. Springer London. ISBN 978-1-4471-0513-8.
- Casey, B., Giedd, J. N., and Thomas, K. M. Structural and functional brain development and its relation to cognitive development. *Biological Psychology*, 54(1):241 – 257, 2000. ISSN 0301-0511. doi: [https://doi.org/10.1016/S0301-0511\(00\)00058-2](https://doi.org/10.1016/S0301-0511(00)00058-2). URL <http://www.sciencedirect.com/science/article/pii/S0301051100000582>.
- Chen, Y., Emer, J., and Sze, V. Eyeriss: A spatial architecture for energy-efficient dataflow for convolutional neural networks. In *2016 ACM/IEEE 43rd Annual International Symposium on Computer Architecture (ISCA)*, pp. 367–379, June 2016. doi: 10.1109/ISCA.2016.40.
- Collins, M. D. and Kohli, P. Memory Bounded Deep Convolutional Networks. *ArXiv e-prints*, December 2014.
- Collins, M. D. and Kohli, P. Memory bounded deep convolutional networks. *CoRR*, abs/1412.1442, 2014. URL <http://arxiv.org/abs/1412.1442>.

- Cortes, C., DeSalvo, G., and Mohri, M. Boosting with abstention. In Lee, D. D., Sugiyama, M., Luxburg, U. V., Guyon, I., and Garnett, R. (eds.), *Advances in Neural Information Processing Systems 29*, pp. 1660–1668. Curran Associates, Inc., 2016. URL <http://papers.nips.cc/paper/6336-boosting-with-abstention.pdf>.
- Courbariaux, M., Bengio, Y., and David, J.-P. Training deep neural networks with low precision multiplications. *arXiv e-prints*, art. arXiv:1412.7024, Dec 2014.
- Cun, Y. L., Denker, J. S., and Solla, S. A. Optimal brain damage. In *Advances in Neural Information Processing Systems*, pp. 598–605. Morgan Kaufmann, 1990.
- D’Agostino, R. B. and Stephens, M. A. (eds.). *Goodness-of-fit Techniques*. Marcel Dekker, Inc., New York, NY, USA, 1986. ISBN 0-824-77487-6.
- Deng, J., Dong, W., Socher, R., Li, L.-J., Li, K., and Fei-Fei, L. ImageNet: A Large-Scale Hierarchical Image Database. In *CVPR09*, 2009.
- Evcı, U., Gale, T., Menick, J., Castro, P. S., and Elsen, E. Rigging the lottery: Making all tickets winners, 2019.
- Feldman, V. and Zhang, C. What Neural Networks Memorize and Why: Discovering the Long Tail via Influence Estimation. *arXiv e-prints*, art. arXiv:2008.03703, August 2020.
- Gale, T., Elsen, E., and Hooker, S. The state of sparsity in deep neural networks. *CoRR*, abs/1902.09574, 2019. URL <http://arxiv.org/abs/1902.09574>.
- Gordon, A., Eban, E., Nachum, O., Chen, B., Wu, H., Yang, T.-J., and Choi, E. Morphnet: Fast & simple resource-constrained structure learning of deep networks. *2018 IEEE/CVF Conference on Computer Vision and Pattern Recognition*, Jun 2018. doi: 10.1109/cvpr.2018.00171. URL <http://dx.doi.org/10.1109/CVPR.2018.00171>.
- Guo, C., Pleiss, G., Sun, Y., and Weinberger, K. Q. On Calibration of Modern Neural Networks. *arXiv e-prints*, art. arXiv:1706.04599, Jun 2017.
- Guo, Y., Yao, A., and Chen, Y. Dynamic network surgery for efficient dnns. *CoRR*, abs/1608.04493, 2016. URL <http://arxiv.org/abs/1608.04493>.
- Guo, Y., Zhang, C., Zhang, C., and Chen, Y. Sparse dnns with improved adversarial robustness. In Bengio, S., Wallach, H., Larochelle, H., Grauman, K., Cesa-Bianchi, N., and Garnett, R. (eds.), *Advances in Neural Information Processing Systems 31*, pp. 242–251. Curran Associates, Inc., 2018. URL <http://papers.nips.cc/paper/7308-sparse-dnns-with-improved-adversarial-robustness.pdf>.
- Gupta, S., Agrawal, A., Gopalakrishnan, K., and Narayanan, P. Deep learning with limited numerical precision. *CoRR*, abs/1502.02551, 2015. URL <http://arxiv.org/abs/1502.02551>.
- Han, S., Pool, J., Tran, J., and Dally, W. J. Learning both Weights and Connections for Efficient Neural Network. In *NIPS*, pp. 1135–1143, 2015.
- Hassibi, B., Stork, D. G., and Com, S. C. R. Second order derivatives for network pruning: Optimal brain surgeon. In *Advances in Neural Information Processing Systems 5*, pp. 164–171. Morgan Kaufmann, 1993a.
- Hassibi, B., Stork, D. G., and Wolff, G. J. Optimal brain surgeon and general network pruning. In *IEEE International Conference on Neural Networks*, pp. 293–299 vol.1, March 1993b. doi: 10.1109/ICNN.1993.298572.
- He, K., Zhang, X., Ren, S., and Sun, J. Deep Residual Learning for Image Recognition. *ArXiv e-prints*, December 2015.
- Hendrycks, D. and Dietterich, T. Benchmarking neural network robustness to common corruptions and perturbations. In *International Conference on Learning Representations*, 2019. URL <https://openreview.net/forum?id=HJz6tiCqYm>.
- Hendrycks, D., Zhao, K., Basart, S., Steinhardt, J., and Song, D. Natural Adversarial Examples. *arXiv e-prints*, art. arXiv:1907.07174, Jul 2019.

- Hinton, G., Vinyals, O., and Dean, J. Distilling the Knowledge in a Neural Network. *arXiv e-prints*, art. arXiv:1503.02531, Mar 2015.
- Hooker, S., Erhan, D., Kindermans, P.-J., and Kim, B. A benchmark for interpretability methods in deep neural networks. In *NeurIPS 2019*, 2019.
- Howard, A. G., Zhu, M., Chen, B., Kalenichenko, D., Wang, W., Weyand, T., Andreetto, M., and Adam, H. MobileNets: Efficient Convolutional Neural Networks for Mobile Vision Applications. *ArXiv e-prints*, April 2017.
- Hubara, I., Courbariaux, M., Soudry, D., El-Yaniv, R., and Bengio, Y. Quantized neural networks: Training neural networks with low precision weights and activations. *CoRR*, abs/1609.07061, 2016. URL <http://arxiv.org/abs/1609.07061>.
- Huber-Carol, C., Balakrishnan, N., Nikulin, M., and Mesbah, M. *Goodness-of-Fit Tests and Model Validity*. Goodness-of-fit Tests and Model Validity. Birkhäuser Boston, 2002. ISBN 9780817642099. URL https://books.google.com/books?id=gUMcv2_NrhkC.
- Iandola, F. N., Han, S., Moskewicz, M. W., Ashraf, K., Dally, W. J., and Keutzer, K. SqueezeNet: AlexNet-level accuracy with 50x fewer parameters and <0.5MB model size. *ArXiv e-prints*, February 2016.
- Ioffe, S. and Szegedy, C. Batch normalization: Accelerating deep network training by reducing internal covariate shift. *CoRR*, abs/1502.03167, 2015. URL <http://arxiv.org/abs/1502.03167>.
- Jacob, B., Kligys, S., Chen, B., Zhu, M., Tang, M., Howard, A., Adam, H., and Kalenichenko, D. Quantization and training of neural networks for efficient integer-arithmetic-only inference. *2018 IEEE/CVF Conference on Computer Vision and Pattern Recognition*, Jun 2018. doi: 10.1109/cvpr.2018.00286. URL <http://dx.doi.org/10.1109/CVPR.2018.00286>.
- Kalchbrenner, N., Elsen, E., Simonyan, K., Noury, S., Casagrande, N., Lockhart, E., Stimberg, F., van den Oord, A., Dieleman, S., and Kavukcuoglu, K. Efficient Neural Audio Synthesis. In *Proceedings of the 35th International Conference on Machine Learning, ICML 2018, Stockholmsmässan, Stockholm, Sweden, July 10-15, 2018*, pp. 2415–2424, 2018.
- Kendall, A. and Gal, Y. What uncertainties do we need in bayesian deep learning for computer vision? In Guyon, I., Luxburg, U. V., Bengio, S., Wallach, H., Fergus, R., Vishwanathan, S., and Garnett, R. (eds.), *Advances in Neural Information Processing Systems 30*, pp. 5574–5584. Curran Associates, Inc., 2017.
- Kim, B., Khanna, R., and Koyejo, O. O. Examples are not enough, learn to criticize! criticism for interpretability. In Lee, D. D., Sugiyama, M., Luxburg, U. V., Guyon, I., and Garnett, R. (eds.), *Advances in Neural Information Processing Systems 29*, pp. 2280–2288. Curran Associates, Inc., 2016.
- Kolb, B. and Wishaw, I. *Fundamentals of Human Neuropsychology*. A series of books in psychology. Worth Publishers, 2009. ISBN 9780716795865.
- Krizhevsky, A. Learning multiple layers of features from tiny images. *University of Toronto*, 05 2012.
- Kumar, A., Goyal, S., and Varma, M. Resource-efficient machine learning in 2 KB RAM for the internet of things. In Precup, D. and Teh, Y. W. (eds.), *Proceedings of the 34th International Conference on Machine Learning*, volume 70 of *Proceedings of Machine Learning Research*, pp. 1935–1944, International Convention Centre, Sydney, Australia, 06–11 Aug 2017. PMLR. URL <http://proceedings.mlr.press/v70/kumar17a.html>.
- Lattner, C., Amini, M., Bondhugula, U., Cohen, A., Davis, A., Pienaar, J., Riddle, R., Shpeisman, T., Vasilache, N., and Zinenko, O. Mlir: A compiler infrastructure for the end of moore’s law, 2020.
- Lee, N., Ajanthan, T., and Torr, P. H. S. SNIP: single-shot network pruning based on connection sensitivity. *CoRR*, abs/1810.02340, 2018. URL <http://arxiv.org/abs/1810.02340>.
- Leibig, C., Allken, V., Ayhan, M. S., Berens, P., and Wahl, S. Leveraging uncertainty information from deep neural networks for disease detection. *Scientific Reports*, 7, 12 2017. doi: 10.1038/s41598-017-17876-z.
- Li, Z., Wallace, E., Shen, S., Lin, K., Keutzer, K., Klein, D., and Gonzalez, J. E. Train large, then compress: Rethinking model size for efficient training and inference of transformers, 2020.
- Liu, Z., Luo, P., Wang, X., and Tang, X. Deep learning face attributes in the wild. In *Proceedings of International Conference on Computer Vision (ICCV)*, December 2015.

- Liu, Z., Li, J., Shen, Z., Huang, G., Yan, S., and Zhang, C. Learning Efficient Convolutional Networks through Network Slimming. *ArXiv e-prints*, August 2017.
- Louizos, C., Welling, M., and Kingma, D. P. Learning Sparse Neural Networks through L_0 Regularization. *ArXiv e-prints*, December 2017.
- Micikevicius, P., Narang, S., Alben, J., Diamos, G., Elsen, E., Garcia, D., Ginsburg, B., Houston, M., Kuchaiev, O., Venkatesh, G., and Wu, H. Mixed Precision Training. *arXiv e-prints*, art. arXiv:1710.03740, October 2017.
- Narang, S., Elsen, E., Diamos, G., and Sengupta, S. Exploring Sparsity in Recurrent Neural Networks. *arXiv e-prints*, art. arXiv:1704.05119, Apr 2017.
- Nowlan, S. J. and Hinton, G. E. Simplifying neural networks by soft weight-sharing. *Neural Computation*, 4(4):473–493, 1992. doi: 10.1162/neco.1992.4.4.473. URL <https://doi.org/10.1162/neco.1992.4.4.473>.
- Rakic, P., Bourgeois, J.-P., and Goldman-Rakic, P. S. Synaptic development of the cerebral cortex: implications for learning, memory, and mental illness. In Pelt, J. V., Corner, M., Uylings, H., and Silva, F. L. D. (eds.), *The Self-Organizing Brain: From Growth Cones to Functional Networks*, volume 102 of *Progress in Brain Research*, pp. 227 – 243. Elsevier, 1994. doi: [https://doi.org/10.1016/S0079-6123\(08\)60543-9](https://doi.org/10.1016/S0079-6123(08)60543-9). URL <http://www.sciencedirect.com/science/article/pii/S0079612308605439>.
- Reagen, B., Whatmough, P., Adolf, R., Rama, S., Lee, H., Lee, S. K., Hernández-Lobato, J. M., Wei, G., and Brooks, D. Minerva: Enabling low-power, highly-accurate deep neural network accelerators. In *2016 ACM/IEEE 43rd Annual International Symposium on Computer Architecture (ISCA)*, pp. 267–278, June 2016. doi: 10.1109/ISCA.2016.32.
- Samala, R. K., Chan, H.-P., Hadjiiski, L. M., Helvie, M. A., Richter, C., and Cha, K. Evolutionary pruning of transfer learned deep convolutional neural network for breast cancer diagnosis in digital breast tomosynthesis. *Physics in Medicine & Biology*, 63(9):095005, may 2018. doi: 10.1088/1361-6560/aabb5b.
- See, A., Luong, M.-T., and Manning, C. D. Compression of Neural Machine Translation Models via Pruning. *arXiv e-prints*, art. arXiv:1606.09274, Jun 2016.
- Sehwag, V., Wang, S., Mittal, P., and Jana, S. Towards compact and robust deep neural networks. *CoRR*, abs/1906.06110, 2019. URL <http://arxiv.org/abs/1906.06110>.
- Sowell, E. R., Thompson, P. M., Leonard, C. M., Welcome, S. E., Kan, E., and Toga, A. W. Longitudinal mapping of cortical thickness and brain growth in normal children. *Journal of Neuroscience*, 24(38): 8223–8231, 2004. doi: 10.1523/JNEUROSCI.1798-04.2004. URL <https://www.jneurosci.org/content/24/38/8223>.
- Strubell, E., Ganesh, A., and McCallum, A. Energy and Policy Considerations for Deep Learning in NLP. *arXiv e-prints*, art. arXiv:1906.02243, June 2019.
- Ström, N. Sparse connection and pruning in large dynamic artificial neural networks, 1997.
- Tessera, K., Hooker, S., and Rosman, B. Keep the gradients flowing: Using gradient flow to study sparse network optimization. *CoRR*, abs/2102.01670, 2021. URL <https://arxiv.org/abs/2102.01670>.
- Theis, L., Korshunova, I., Tejani, A., and Huszár, F. Faster gaze prediction with dense networks and Fisher pruning. *CoRR*, abs/1801.05787, 2018. URL <http://arxiv.org/abs/1801.05787>.
- Ullrich, K., Meeds, E., and Welling, M. Soft Weight-Sharing for Neural Network Compression. *CoRR*, abs/1702.04008, 2017.
- Valin, J. and Skoglund, J. Lpcnet: Improving Neural Speech Synthesis Through Linear Prediction. *CoRR*, abs/1810.11846, 2018. URL <http://arxiv.org/abs/1810.11846>.
- Vanhoucke, V., Senior, A., and Mao, M. Z. Improving the speed of neural networks on cpus. In *Deep Learning and Unsupervised Feature Learning Workshop, NIPS 2011*, 2011.
- Weigend, A. S., Rumelhart, D. E., and Huberman, B. A. Generalization by weight-elimination with application to forecasting. In Lippmann, R. P., Moody, J. E., and Touretzky, D. S. (eds.), *Advances in Neural Information Processing Systems 3*, pp. 875–882. Morgan-Kaufmann, 1991.

- Welch, B. L. The generalization of ‘Student’s’ problem when several different population variances are involved. *Biometrika*, 34:28–35, 1947. ISSN 0006-3444. doi: 10.2307/2332510. URL <https://doi.org/10.2307/2332510>.
- Wen, W., Wu, C., Wang, Y., Chen, Y., and Li, H. Learning Structured Sparsity in Deep Neural Networks. *ArXiv e-prints*, August 2016.
- Zagoruyko, S. and Komodakis, N. Wide residual networks. *CoRR*, abs/1605.07146, 2016. URL <http://arxiv.org/abs/1605.07146>.
- Zech, J. R., Badgeley, M. A., Liu, M., Costa, A. B., Titano, J. J., and Oermann, E. K. Variable generalization performance of a deep learning model to detect pneumonia in chest radiographs: A cross-sectional study. *PLOS Medicine*, 15(11):1–17, 11 2018. doi: 10.1371/journal.pmed.1002683. URL <https://doi.org/10.1371/journal.pmed.1002683>.
- Zhang, J. Selecting typical instances in instance-based learning. In Sleeman, D. and Edwards, P. (eds.), *Machine Learning Proceedings 1992*, pp. 470 – 479. Morgan Kaufmann, San Francisco (CA), 1992. ISBN 978-1-55860-247-2. doi: <https://doi.org/10.1016/B978-1-55860-247-2.50066-8>. URL <http://www.sciencedirect.com/science/article/pii/B9781558602472500668>.
- Zhou, W., Veitch, V., Austern, M., Adams, R. P., and Orbanz, P. Non-vacuous generalization bounds at the imagenet scale: a pac-bayesian compression approach. In *ICLR*, 2019.
- Zhu, M. and Gupta, S. To prune, or not to prune: exploring the efficacy of pruning for model compression. *ArXiv e-prints*, October 2017.
- Zhu, M. and Gupta, S. To prune, or not to prune: exploring the efficacy of pruning for model compression. *CoRR*, abs/1710.01878, 2017a. URL <http://arxiv.org/abs/1710.01878>.
- Zhu, M. and Gupta, S. To prune, or not to prune: exploring the efficacy of pruning for model compression, 2017b.

Appendix

A Pruning and quantization techniques considered

Magnitude pruning There are various pruning methodologies that use the absolute value of weights to rank their importance and remove weights that are below a user-specified threshold (Collins & Kohli, 2014; Guo et al., 2016; Zhu & Gupta, 2017a). These works largely differ in whether the weights are removed permanently or can “recover” by still receiving subsequent gradient updates. This would allow certain weights to become non-zero again if pruned incorrectly. While magnitude pruning is often used as a criteria to remove individual weights, it can be adapted to remove entire neurons or filters by extending the ranking criteria to a set of weights and setting the threshold appropriately (Gordon et al., 2018).

In this work, we use the magnitude pruning methodology as proposed by Zhu & Gupta (2017a). It has been shown to outperform more sophisticated Bayesian pruning methods and is considered state-of-the-art across both computer vision and language models (Gale et al., 2019). The choice of magnitude pruning also allowed us to specify and precisely vary the final model sparsity for purposes of our analysis, unlike regularizer approaches that allow the optimization process itself to determine the final level of sparsity (Liu et al., 2017; Louizos et al., 2017; Collins & Kohli, 2014; Wen et al., 2016; Weigend et al., 1991; Nowlan & Hinton, 1992).

Quantization All networks were trained with 32-bit floating point weights and quantized post-training. This means there is no additional gradient updates to the weights post-quantization. In this work, we evaluate three different quantization methods. The first type replaces the weights with 16-bit floating point weights (Micikevicius et al., 2017). The second type quantizes all weights to 8-bit integer values (Alvarez et al., 2016). The third type uses the first 100 training examples of each dataset as representative examples for the fixed-point only models. We chose to benchmark these quantization methods in part because each has open source code available. We use TensorFlow Lite with MLIR (Lattner et al., 2020).

B Pruning Protocol

We prune over the course of training to obtain a target end pruning level $t \in \{0.0, 0.1, 0.3, 0.5, 0.7, 0.9\}$. Removed weights continue to receive gradient updates after being pruned. These hyperparameter choices were based upon a limited grid search which suggested that these particular settings minimized degradation to test-set accuracy across all pruning levels. We note that for CelebA we were able to still converge to a comparable final performance at much higher levels of pruning $t \in \{0.95, 0.99\}$. We include these results, and note that the tolerance for extremely high levels of pruning may be related the relative difficulty of the task. Unlike CIFAR-10 and ImageNet which involve more than 2 classes (10 and 1000 respectively), CelebA is a binary classification problem. Here, the task is predicting hair color $Y = \{\text{blonde, dark haired}\}$.

Quantization techniques are applied post-training - the weights are not re-calibrated after quantizing. Figure 1 shows the distributions of model accuracy across model populations for the pruned and quantized models for ImageNet, CIFAR-10 and CelebA. Table. 4 and Table. 5 include top-line metrics for all compression methods considered.

C Human study

We conducted a human study (involving 85 volunteers) to label a random sample of 1230 PIE and non-PIE ImageNet images. Humans in the study were shown a balanced sample of PIE and non-PIE images that were selected at random and shuffled. The classification as PIE or non-PIE was not known or available to the human. Participants answered the following questions for each image that was presented:

- *Does label 1 accurately label an object in the image? (0/1)*
- *Does this image depict a single object? (0/1)*
- *Would you consider labels 1, 2 and 3 to be semantically very close to each other? (does this image require fine grained classification) (0/1)*

ImageNet Robustness to ImageNet-C Corruptions (By Level of Pruning)					
Pruning Fraction	Corruption Type	Top-1	Top-5	Top-1 Norm	Top-5 Norm
0.0	brightness	69.49	88.98	0.00	0.00
0.7	brightness	67.50	87.86	-2.87	-1.25
0.9	brightness	64.12	85.63	-7.74	-3.77
0.0	contrast	42.30	61.80	0.00	0.00
0.7	contrast	41.34	61.58	-2.26	-0.36
0.9	contrast	38.04	58.43	-10.06	-5.45
0.0	defocus_blur	49.77	72.45	0.00	0.00
0.7	defocus_blur	47.49	70.69	-4.58	-2.43
0.9	defocus_blur	44.69	68.26	-10.22	-5.79
0.0	elastic	57.09	76.71	0.00	0.00
0.7	elastic	55.09	75.29	-3.51	-1.85
0.9	elastic	52.81	73.62	-7.50	-4.02
0.0	fog	56.21	79.25	0.00	0.00
0.7	fog	54.46	78.25	-3.12	-1.25
0.9	fog	50.36	75.10	-10.41	-5.23
0.0	frosted_glass_blur	40.89	60.51	0.00	0.00
0.7	frosted_glass_blur	38.75	58.68	-5.23	-3.03
0.9	frosted_glass_blur	36.87	57.02	-9.83	-5.78
0.0	gaussian_noise	45.43	65.67	0.00	0.00
0.7	gaussian_noise	42.01	62.40	-7.53	-4.98
0.9	gaussian_noise	32.88	51.49	-27.64	-21.59
0.0	impulse_noise	42.23	63.16	0.00	0.00
0.7	impulse_noise	37.91	58.82	-10.24	-6.87
0.9	impulse_noise	25.29	43.13	-40.12	-31.70
0.0	jpeg_compression	65.75	86.25	0.00	0.00
0.7	jpeg_compression	63.47	84.81	-3.47	-1.68
0.9	jpeg_compression	60.57	82.77	-7.88	-4.04
0.0	pixelate	57.34	78.05	0.00	0.00
0.7	pixelate	54.93	76.17	-4.21	-2.41
0.9	pixelate	51.31	72.98	-10.51	-6.50
0.0	shot_noise	43.82	64.06	0.00	0.00
0.7	shot_noise	39.88	60.04	-8.99	-6.28
0.9	shot_noise	30.80	48.86	-29.71	-23.72
0.0	zoom_blur	37.16	58.90	0.00	0.00
0.7	zoom_blur	34.60	56.68	-6.89	-3.76
0.9	zoom_blur	31.78	53.97	-14.47	-8.37

Table 3: Pruned models are more sensitive to image corruptions that are meaningless to a human. We measure the average top-1 and top-5 test set accuracy of models trained to varying levels of pruning on the ImageNet-C test-set (the models were trained on uncorrupted ImageNet). For each corruption type, we report the average accuracy of 50 trained models relative to the baseline models across all 5 levels of pruning.

CelebA		
Fraction Pruned	Top 1	# PIEs
0	94.73	-
0.3	94.75	555
0.5	94.81	638
0.7	94.44	990
0.9	94.07	3229
0.95	93.39	5057
0.99	90.98	8754
Quantization	Top 1	# PIEs
hybrid int8	94.65	404
fixed-point int8	94.65	414

Table 4: CelebA top-1 accuracy at all levels of pruning, averaged over runs. The task we consider for CelebA is a binary classification method. We consider exemplar level divergence and classify Pruning Identified Exemplars as the examples where the modal label differs between a population of 30 compressed and non-compressed models. Note that the CelebA task is a binary classification task to predict whether the celebrity is blond or non-blond. Thus, there are only two classes.

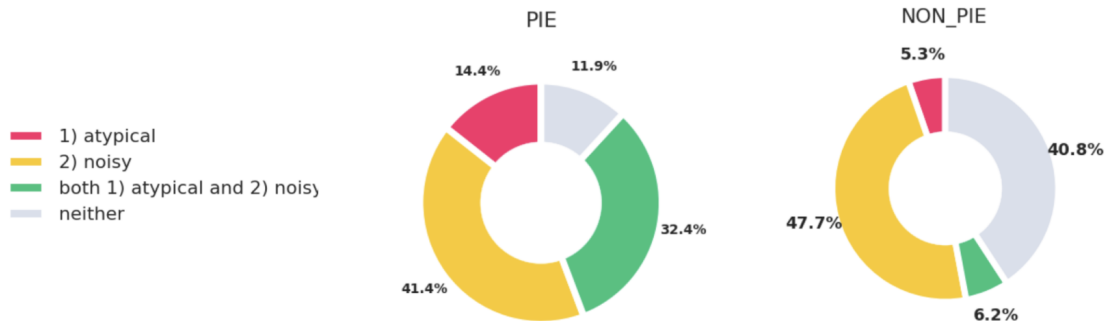


Figure 5: A pie chart of the codified attributes of a sample of pruning identified exemplars (PIEs) and non-PIE images. The human study shows that PIEs over-index on both **noisy** exemplars with partial or corrupted information (corrupted images, incorrect labels, multi-object images) and/or **atypical** or challenging images (abstract representation, fine grained classification).

- *Do you consider the object in the image to be a typical exemplar for the class indicated by label 1?* (0/1)
- *Is the image quality corrupted (some common image corruptions – overlaid text, brightness, contrast, filter, defocus blur, fog, jpeg compression, pixelate, shot noise, zoom blur, black and white vs. rgb)?* (0/1)
- *Is the object in the image an abstract representation of the class indicated by label 1? [[an abstract representation is an object in an abstract form, such as a painting, drawing or rendering using a different material.]]* (0/1)

We find that PIEs heavily over-index relative to non-PIEs on both **noisy** examples with corrupted information (incorrect ground truth label, multiple objects, image corruption) and **atypical** or challenging examples (fine-grained classification task, abstract representation). We include the per attribute relative representation of PIE vs. Non-PIE for the study (in Figure. 7).

ImageNet			
Fraction Pruned	Top 1	# Signif classes	# PIEs
0	76.68	-	-
30	76.46	68	1,819
50	75.87	170	2,193
70	75.02	372	3,073
90	72.60	637	5,136
Quantization			
float16	76.65	58	2019
dynamic range int8	76.10	144	2193
fixed-point int8	76.46	119	2093
CIFAR-10			
Fraction Pruned	Top 1	# Signif classes	# PIEs
0	94.53	-	-
30	94.47	1	114
50	94.39	1	144
70	94.30	0	137
90	94.14	2	216

Table 5: CIFAR-10 and ImageNet top-1 accuracy at all levels of pruning, averaged over 30 runs. Top-5 accuracy for CIFAR-10 was 99.8% for all levels of pruning. The third column is the number of classes significantly impacted by pruning.

D Benchmarks to evaluate robustness

ImageNet-A Extended Results ImageNet-A is a curated test set of 7, 500 natural adversarial images designed to produce drastically low test accuracy. We find that the sensitivity of pruned models to ImageNet-A mirrors the patterns of degradation to ImageNet-C and sets of PIEs. As pruning increases, top-1 and top-5 accuracy further erode, suggesting that pruned models are more brittle to adversarial examples. Table 8 includes relative and absolute sensitivity at all levels of compression considered.

For each robustness benchmark and level of pruning that we evaluate, we average model robustness over 5 models independently trained from random initialization.



Figure 6: Visualization of Pruning Identified Exemplars from the CIFAR-10 dataset. This subset of impacted images is identified by considering a set of 30 non-pruned wide ResNet models and 30 models trained to 30% pruning. Below each image are three labels: 1) true label, 2) the modal (most frequent) prediction from the set of non-pruned models, 3) the modal prediction from the set of pruned models.

Top-1 accuracy				Top-5 accuracy		
ImageNet						
Fraction Pruned	Non-PIEs	PIEs	All	Non-PIEs	PIEs	All
10.0	79.34	26.14	76.75	94.89	68.52	93.35
30.0	79.23	26.21	76.75	95.04	69.30	93.35
50.0	79.54	28.74	76.75	94.89	71.47	93.35
70.0	80.16	32.06	76.75	94.99	74.74	93.35
90.0	81.20	39.81	76.75	95.11	78.90	93.35
CIFAR-10						
Fraction Pruned	Non-PIEs	PIEs	All	Non-PIEs	PIEs	All
10.0	95.11	43.23	94.89	99.91	95.30	99.91
30.0	95.40	40.61	94.89	99.92	92.83	99.91
50.0	95.45	40.42	94.89	99.93	93.53	99.91
70.0	95.56	43.64	94.89	99.94	95.95	99.91
90.0	95.60	50.71	94.89	99.92	96.67	99.91
CelebA						
Fraction Pruned	Non-PIEs	PIEs	All	Non-PIEs	PIEs	All
30.0	94.76	49.82	94.76	-	-	-
50.0	94.78	50.55	94.78	-	-	-
70.0	94.54	52.61	94.54	-	-	-
90.0	94.10	50.41	94.10	-	-	-
95.0	93.40	45.57	93.40	-	-	-
99.0	90.97	39.84	90.97	-	-	-

Table 6: A comparison of non-compressed model performance on Pruning Identified Exemplars (PIE) relative to a random sample drawn independently from the test-set and a sample excluding PIEs (non-PIEs). Inference on the non-PIE sample improves test-set top-1 accuracy relative to the baseline for ImageNet and Cifar-10. Evaluation on PIE images alone yields substantially lower top-1 accuracy. Note that CelebA top-5 is not included as it is a binary classification problem.

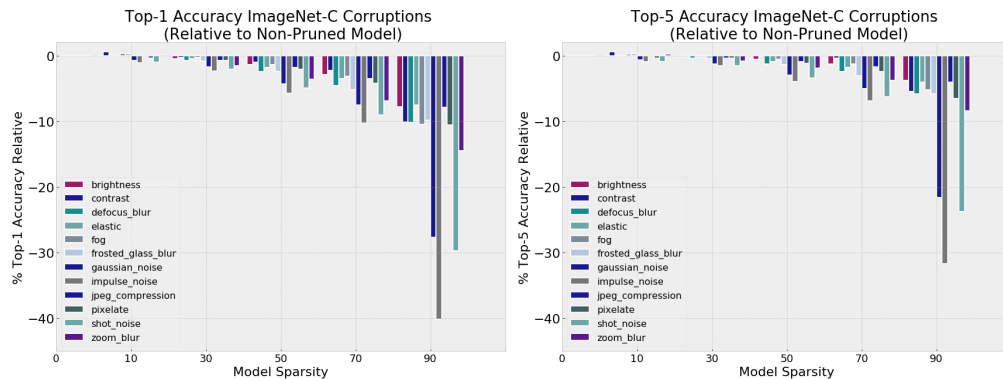


Figure 7: High levels of compression amplify sensitivity to distribution shift. **Left:** Change to top-1 normalized recall of a pruned model **relative** to a non-pruned model on ImageNet-C (all corruptions). **Right:** Change to top-5 normalized recall of a pruned model **relative** to a non-pruned model on ImageNet-C (all corruptions). We measure the top-1 test-set performance on a subset of ImageNet-C corruptions of a pruned model **relative** to the non-pruned model on the same corruption.

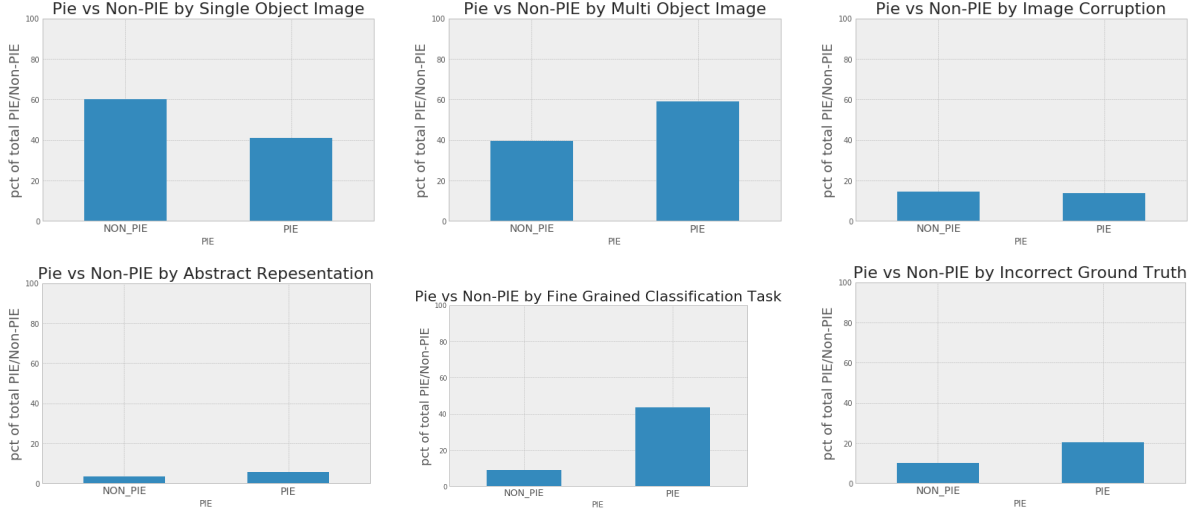


Table 7: PIE vs non-PIE relative representation for different attributes. These attributes were codified in a human study involving 85 individuals inspecting a balanced random sample of PIE and non-PIE. The classification as PIE or non-PIE was not known or available to the human.

ImageNet Robustness to ImageNet-A Corruptions (By Level of Pruning)				
Pruning Fraction	Top-1	Top-5	Top-1 Norm	Top-5 Norm
0.0	0.89	7.56	0.00	0.00
10.0	0.85	7.53	-4.04	-0.39
30.0	0.76	7.21	-14.33	-4.62
50.0	0.62	6.53	-30.54	-13.65
70.0	0.51	5.83	-42.63	-22.96
90.0	0.36	4.47	-59.80	-40.96

Table 8: Pruned models are more sensitive to natural adversarial images. ImageNet-A is a curated test set of 7,500 natural adversarial images designed to produce drastically low test accuracy. We compute the absolute performance of models pruned to different levels of sparsity on ImageNet-A (Top-1 and Top-5) as well as the normalized performance relative to a non-pruned model on ImageNet-A.

ImageNet-C Extended Results ImageNet-C (Hendrycks & Dietterich, 2019) is an open source data set that consists of algorithmic generated corruptions (blur, noise) applied to the ImageNet test-set. We compare top-1 accuracy given inputs with corruptions of different severity. As described by the methodology of Hendrycks & Dietterich (2019), we compute the corruption error for each type of corruption by measuring model performance rate across five corruption severity levels (in our implementation, we normalize the per-corruption error by the performance of the non-compressed model on the same corruption).

ImageNet-C corruption substantially degrades mean top-1 accuracy of pruned models relative to non-pruned. As seen in Fig.7, this sensitivity is amplified at high levels of pruning, where there is a further steep decline in top-1 accuracy. Unlike the main body, in this figure we visualize all corruption types considered. Sensitivity to different corruptions is remarkably varied, with certain corruptions such as Gaussian, shot an impulse noise consistently causing more degradation. We include a visualization for a larger sample of corruptions considered in Table 3.